Angular steering of the free-electron-laser far-field radiation beam

Eli Jerby
Faculty of Engineering, Tel Aviv University, Ramat Aviv 69978, Israel
and Research Laboratory of Electronics, Massachusetts Institute of Technology, Cambridge, Massachusetts 02139
(Received 2 November 1989)

The free-electron laser (FEL) is presented theoretically in this paper as an angularly directed radiation source. Features of phased-array antenna are incorporated in known FEL schemes to provide the angular steering of the FEL radiation in the far field. Various methods for FEL angular steering are proposed. These are classified in this paper as *end-fire* and *broadside* schemes. A unified two-dimensional linear model for the FEL angular steering is derived and implemented to demonstrate the performances of the various steering methods. It is shown that by using a miniature wiggler, a considerable angular steering range is feasible in the broadside FEL scheme in the *millimeter* wave range. Possible applications for the FEL angular steering features, considering their limitations, are proposed.

I. INTRODUCTION

Free-electron lasers (FEL) are well known as sources and amplifiers for em radiation. They are operated in a wide spectrum of frequencies, from microwaves to ultraviolet wavelengths. The tunability range of a FEL may exceed a full octave, and its output power is usually high.[1,2] This paper presents a theoretical study of another possible feature of the FEL—the theoretical possibility of angular steering of the FEL output radiation beam in the far field. Various techniques are studied to achieve off-axis radiation lobe in the far field for a high-gain FEL, and for optical klystron (prebunched FEL).

The FEL is presented in this paper as a directed radiation source, as shown schematically in Fig. 1. This approach leads to a scheme of a hybrid FEL-antenna system. It is shown here that an appropriate modification of the FEL (phase) detuning conditions may result in angular steering of the output radiation beam, as in the known *phased-array antennas*,[3] in which the angular steering is performed by electronic control on the relative phase shift of each radiating element in the array. The practical importance of the phased-array antennas for radar and other applications stems from the alleviation of the need for mechanical systems to steer the radiation beam; hence the angular steering becomes faster and simpler. The FEL antenna hybrid may have a similar advantage, in addition to the simplicity that may be achieved by combining the two functions, the radiation source and the antenna, in one hybrid device.

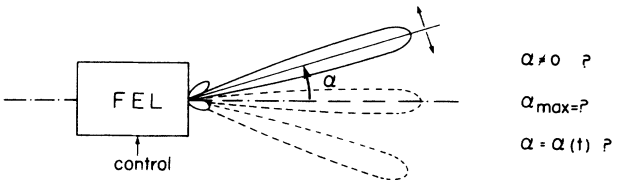

FIG. 1. The angular steering free electron laser. The off-axis angle of the radiation lobe α is controlled by variation of the FEL parameters.

Aspects of the FEL operating features relevant to various angular steering mechanisms have been investigated by other workers. Sprangle *et al.*[4] studied the radiation focusing and guiding in free-electron lasers, and presented the possibility of steering the radiation beam by bending the electron (e) beam. Colson *et al.*[5] extended the theory of free-electron lasers to include the angular gain spectrum. The analysis of the angular steering in the high-gain FEL schemes is strongly related to the *optical guiding* feature of the FEL, and to the evolution of a modified phase profile at the exit of the FEL interaction. These subjects have been studied theoretically[6,7] and experimentally[8–10] for systems with transverse symmetry. In the present work we extend the optical guiding feature to asymmetrical systems to create the off-axis radiation beam in the far field, as described later. Other schemes of angular steering are related to optical klystron[11,12] and to prebunched FEL's.[13–15] A linear one-dimensional (1D) model for the prebunched FEL, derived by Schnitzer and Gover,[13] results in a nonzero initial value expansion of the ordinary FEL gain-dispersion equation.[16,17] This is extended here to a two-dimensional model, including transversely nonuniform e-beam profiles. A *transfer function* for the prebunched FEL, in the form of the matrix gain-dispersion equations of Ref. 18, is derived. It is used here to study the angular steering effect in the various schemes. The parametric regime that corresponds to the microwiggler concept,[19] namely short wiggler period and low e-beam energy, is found attractive for the angular steering FEL operation.

II. PRINCIPLES OF ANGULAR STEERING SCHEMES

The various beam steering mechanisms studied in this paper are classified, in terms of antenna arrays, as *end-*

fire and *broadside* FEL radiators.[3]

The end-fire steering corresponds to a high-gain FEL in which the radiation is confined to the e beam, and is emitted from the FEL exit plane with a nonuniform (and asymmetrical) phase profile. This effect can be achieved by introducing a transverse asymmetry to the FEL parameters, as shown in Fig. 2(a). The FEL employs in this case a wide e beam (or a multiple e beam). The transverse shear in the e-beam axial velocity at the entrance leads to a transverse shear in the FEL synchronism condition $\bar{\theta}$. The FEL acceptance of a synchronism detuning in the high-gain regime is of the order of a few periods $[\Delta\bar{\theta}\sim(2-6)\pi]$.[17] Consequently, the phase profile of the emitted electromagnetic wave (at the exit plane of the FEL) acquires a similar shear. This phase shear causes the angular deviation of the FEL radiation beam in the far field. Hence, by inducing a small velocity shear in the e beam one may steer the radiation emitted off axis in the far field. Transverse shears in other FEL parameters, such as the e-beam density or the wiggler strength, may enhance the effect in some cases, and may also compensate for the FEL detuning due to the velocity shear.

The method of broadside steering corresponds to a device similar to the known optical klystron. It consists of a buncher (a FEL section) and a broadside radiator (a prebunched FEL) as shown in Fig. 2(b). The angular steering is achieved by a longitudinal modification of the detuning parameter. This can be done in a third section, between the buncher and the radiator, by adding a small amount of energy ΔE to the bunched e beam as shown in Fig. 2(b). The broadside steering effect can be explained in a simplified manner as follows. The optimal synchronism condition for a single plane wave in a free electron laser is given by the relation[16]

$$\bar{\theta}=(\omega/V_z-k_z-k_W)L_W\sim 0 \tag{1}$$

where k_z, the axial component of the wave-number vector $\mathbf{k}=(\mathbf{k}_\perp,\hat{\mathbf{z}}k_z)$, is given by $k_z=(|\mathbf{k}|^2-|\mathbf{k}_\perp|^2)^{1/2}$, and ω is the angular frequency, V_z is the average e-beam axial velocity, $k_W=2\pi/\lambda_W$ is the wiggler wave number, and L_W is the wiggler length. In general, the plane wave interacting with the FEL is not necessarily propagating on axis. The off-axis angle of propagation is given by the ratio between the transverse and the axial wave-number components,

$$\alpha=\arctan(|\mathbf{k}_\perp|/k_z)\ . \tag{2}$$

These relations can be presented figuratively, as shown in Fig. 3, by modifying the FEL synchronism diagrams[16] to include the off-axis angle of propagation α. The simplified presentation of the FEL steering feature in Fig. 3, row (b), shows that the off-axis angle is increased by increasing the prebunched e-beam velocity V_z, at the same prebunched frequency ω. A similar effect is obtained if, instead of increasing the prebunched e-beam energy, the wiggler period at the radiation section is made shorter than that of the buncher section. This case is shown in Fig. 3, row (c). Hence, modifying the wiggler periodicity is another way to obtain angular steering in a broadside

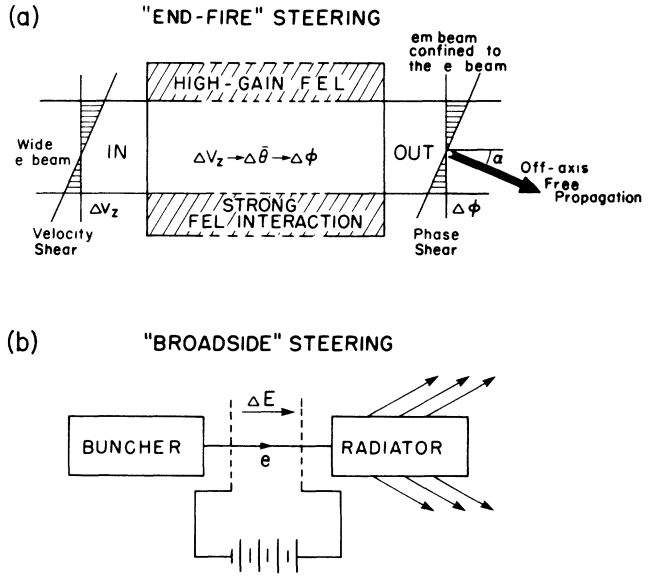

FIG. 2. Schematic description of angular steering methods. (a) the end-fire scheme for high-gain FEL—a small transverse velocity shear of the e-beam axial velocity V_z results in a transverse shear of the detuning condition, $\bar{\theta}$. Consequently, it leads to a slated phase profile $\Delta\phi$ at the FEL exit plane, and to an off-axis propagation of the radiation beam in the free space. (b) The broadside scheme for a prebunched FEL—by a small increase in the energy of the prebunched e beam ("bunch stretching") the radiator emits off-axis radiation beam.

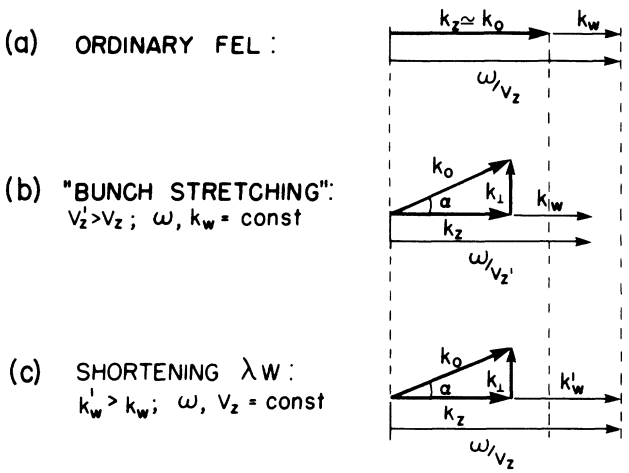

FIG. 3. Synchronism diagrams for the broadside angular steering schemes. In the ordinary FEL (a) the e beam, the wiggler, and the radiation beam are coaxial. In the "bunch stretching" mechanism (b) the prebunched e-beam velocity is increased and consequently α, the off-axis radiation angle, grows. The same effect occurs if the wiggler periodicity in the radiator section is shortened (c).

scheme. Its practical feasibility is limited, however, to electromagnetic wave wigglers in which the wavelength can be tuned.

The heuristic explanation for the angular steering given above is based on a single plane-wave FEL interaction. For an accurate description of a transversely finite FEL, one should incorporate the effect of a wider spectrum of plane waves within the acceptance range of the FEL interaction. This is done in the next section.

III. UNIFIED 2D MODEL OF PREBUNCHED, TRANSVERSELY NONUNIFORM FEL

The analysis of the various FEL angular steering schemes is done by a simplified version of the 3D kinetic model presented in Ref. 18. This model is reduced here to a 2D fluid model. It is extended to include initial prebunching of the e beam, and transverse shears in the velocity and density profiles of the e beam. The model derived here is applicable therefore for both the end-fire and the broadside schemes.

An ideal planar wiggler field, $\mathbf{B}_W=\hat{\mathbf{y}}B_{W_y}\sin(k_W z)$, is assumed. The em field components included in the model are $\mathbf{E}=\hat{\mathbf{x}}E_x+\hat{\mathbf{z}}E_z$, and $\mathbf{H}=\hat{\mathbf{y}}H_y$. All the functional dependence is on (x,z) only. After linearization and performing Fourier transform on the time dimension $(\partial/\partial t\rightarrow j\omega)$ the 2D Maxwell equations are written in the form

$$\frac{\partial}{\partial z}\tilde{E}_x-\frac{\partial}{\partial x}\tilde{E}_z=-j\omega\mu_0\tilde{H}_y\ , \tag{3a}$$

$$\frac{\partial}{\partial x}\tilde{E}_x+\frac{\partial}{\partial z}\tilde{E}_z=\tilde{\rho}_1/\epsilon_0\ , \tag{3b}$$

$$-\frac{\partial}{\partial z}\tilde{H}_y=j\omega\epsilon_0\tilde{E}_x+\tilde{J}_x\ , \tag{4a}$$

$$\frac{\partial}{\partial x}\tilde{H}_y=j\omega\epsilon_0\tilde{E}_z+\tilde{J}_z\ . \tag{4b}$$

The first-order current and density components, $\tilde{J}_z$, $\tilde{J}_x$, and $\tilde{\rho}_1$, respectively, are related to the zero- and first-order axial velocity components, V_z and $\tilde{v}_z$, respectively, as follows:

$$\tilde{J}_z=\rho_0\tilde{v}_z+\tilde{\rho}_1V_z\ , \tag{5a}$$

$$\tilde{J}_x\cong\tilde{\rho}_1V_{W_x}\cos(k_W z)\ , \tag{5b}$$

$$\frac{\partial}{\partial x}\tilde{J}_x+\frac{\partial}{\partial z}\tilde{J}_z=-j\omega\tilde{\rho}_1\ . \tag{5c}$$

The wiggling velocity in the x direction is $V_{W_x}\cos(k_W z)$. Its amplitude is given by $V_{W_x}=a_W/\gamma$ where the wiggler parameter is $a_W=eB_{W_y}/mck_W$, and $\gamma_z=\gamma/(1+a_W^2)^{1/2}$. The first-order axial velocity $\tilde{v}_z$ is found by the $\hat{\mathbf{z}}$ component of the first-order Lorentz equation, given in the form

$$j\omega\tilde{v}_z+V_z\frac{\partial}{\partial z}\tilde{v}_z=\frac{-e}{\gamma\gamma_z^2m}[\tilde{E}_z+\mu_0V_{W_x}\tilde{H}_y\cos(k_W z)]\ . \tag{6}$$

A self-consistent set of algebraic equations is obtained by Laplace transform, performed on the $\hat{\mathbf{z}}$ dimension, namely, $\tilde{\tilde{\rho}}_1(s)=\mathcal{L}(\tilde{\rho}_1(z))=\int_z\tilde{\rho}_1(z)\exp(-sz)dz$, as in Ref. 18. Equations (3)–(6) are written in the s plane in the form

$$s\tilde{\tilde{H}}_y-\tilde{H}_{y0}=-j\omega\epsilon_0\tilde{\tilde{E}}_x-\tilde{\tilde{J}}_x\ , \tag{7a}$$

$$s\tilde{\tilde{E}}_x-E_{x0}=\frac{\partial}{\partial x}\tilde{\tilde{E}}_z-j\omega\mu_0\tilde{\tilde{H}}_y\ , \tag{7b}$$

$$s\tilde{\tilde{E}}_z-\tilde{E}_{z0}=-\frac{\partial}{\partial x}\tilde{\tilde{E}}_x+\tilde{\tilde{\rho}}_1/\epsilon_0\ , \tag{7c}$$

$$j\omega\epsilon_0\tilde{\tilde{E}}_z=\frac{\partial}{\partial x}\tilde{\tilde{H}}_y-\tilde{\tilde{J}}_z\ , \tag{7d}$$

$$\tilde{\tilde{J}}_z=\rho_0\tilde{\tilde{v}}_z+\tilde{\tilde{\rho}}_1V_z\ , \tag{7e}$$

$$\tilde{\tilde{J}}_x=\tfrac{1}{2}V_{W_x}(\tilde{\tilde{\rho}}^{(+1)}+\tilde{\tilde{\rho}}^{(-1)})\ , \tag{7f}$$

$$s\tilde{\tilde{J}}_z-\tilde{J}_{z0}=-\frac{\partial}{\partial x}\tilde{\tilde{J}}_x-j\omega\tilde{\tilde{\rho}}_1\ , \tag{7g}$$

and

$$(j\omega+V_zs)\tilde{\tilde{v}}_z=V_z\tilde{v}_{z0}-\frac{e}{\gamma\gamma_z^2m}[\tilde{\tilde{E}}_z+\tfrac{1}{2}\mu_0V_{W_x}(\tilde{\tilde{H}}_y^{(+1)}+\tilde{\tilde{H}}_y^{(-1)})]\ . \tag{7h}$$

The (±1) indexing corresponds to $\pm jk_W$ modulation in the s plane, namely, $\tilde{\tilde{\rho}}_1^{(+1)}=\tilde{\tilde{\rho}}_1(s+jk_W)$.

For an ordinary FEL the initial conditions for the current sources can be considered as zero, namely $\tilde{J}_{z0}=\tilde{v}_{z0}=0$.[18] However, in order to incorporate the nonzero initial conditions for the prebunched FEL schemes, we assume as in Ref. 13 that

$$\tilde{J}_{z0},\quad \tilde{v}_{z0}\neq0\ . \tag{8}$$

Using the free-space relation, $jk_z\tilde{E}_{x0}=j\omega\mu_0\tilde{H}_{y0}$, and performing some algebraic operations, Eqs. (7a)–(7h) are further developed to the approximated form

$$\left[k^2+s^2+\left(\frac{\partial}{\partial x}\right)^2\right]\tilde{\tilde{E}}_x^{(0)}-2s\tilde{E}_{x0}=j\omega\mu_0\tilde{\tilde{J}}_x^{(0)}\ , \tag{9a}$$

$$\tilde{\tilde{J}}_x^{(0)}\cong\tfrac{1}{2}V_{W_x}\tilde{\tilde{\rho}}_1^{(-1)}\ , \tag{9b}$$

$$\tilde{\tilde{\rho}}_1^{(-1)}\cong-\frac{s-jk_W}{j\omega}\tilde{\tilde{J}}_z^{(-1)}+\frac{1}{j\omega}\tilde{J}_{z0}\ , \tag{9c}$$

$$\tilde{\tilde{J}}_z^{(-1)}=\frac{1}{1+\chi_z^{(-1)}}\left[-\frac{1}{2}\epsilon_0sV_{W_x}\chi_z^{(-1)}\tilde{\tilde{E}}_x^{(0)}+\frac{j\omega\rho_0V_z\tilde{\tilde{v}}_{z0}}{[j\omega+(s-jk_W)V_z]^2}+\frac{V_z\tilde{J}_{z0}}{j\omega+(s-jk_W)V_z}\right]\ . \tag{9d}$$

The longitudinal e-beam susceptibility term is defined here as

$$\chi_z(x)^{(-1)}=-\frac{e\rho_0(x)}{\gamma\gamma_z^2 m V_z^2\epsilon_0}\frac{1}{[j\omega/V_z(x)+s-jk_W]^2}\ . \quad (10)$$

Note that two different shears are included simultaneously in the susceptibility term $\chi_z(x)$; one is the velocity shear $V_z(x)$ and the other is the density shear $\rho_0(x)$.

Equations (9a)–(9d) result in an ordinary differential equation of the second order,

$$\frac{1}{2s}\frac{d^2}{dx^2}\tilde{\tilde{E}}_x^{(0)}+\left[\frac{1}{2s}(s^2+k^2)+j\kappa\frac{\chi_z^{(-1)}}{1+\chi_z^{(-1)}}\right]\tilde{\tilde{E}}_x^{(0)}$$
$$=\tilde{E}_{x0}+j\frac{kV_{W_x}}{4\bar{v}_z c}\frac{\rho_0}{\epsilon_0\theta_p^2}\frac{\chi_z^{(-1)}}{1+\chi_z^{(-1)}}\tilde{v}_{z0}+\frac{\mu_0 V_{W_x}}{4s}\left[\frac{j\omega/V_z}{j\omega/V_z+s-jk_W}\frac{1}{1+\chi_z^{(-1)}}+\frac{\chi_z^{(-1)}}{1+\chi_z^{(-1)}}\right]\tilde{J}_{z0}\ , \quad (11)$$

where the FEL coupling parameter is defined as

$$\kappa=\frac{kV_{W_x}^2}{8\bar{v}_z c}=\frac{k}{8\bar{\beta}_z}\left[\frac{a_W}{\gamma}\right]^2 \quad (12)$$

and $\theta_p=[e\rho_0(x)/(\gamma\gamma_z^2 m V_z^2\epsilon_0)]^{1/2}$ is the space-charge parameter.[16] Equation (11) is rewritten in the simplified form

$$\frac{1}{2s}\frac{d^2}{dx^2}\tilde{\tilde{E}}_x^{(0)}(x)+\left[\frac{1}{2s}(k^2+s^2)+j\kappa\tilde{\tilde{D}}(x)\right]\tilde{\tilde{E}}_x^{(0)}(x)$$
$$=\tilde{E}_{x0}(x)+j\zeta\tilde{\tilde{D}}(x)\tilde{J}_{\rm in}\ . \quad (13)$$

The dispersion coefficient $\tilde{\tilde{D}}$ is defined here as

$$\tilde{\tilde{D}}=\frac{\chi_z^{(-1)}}{1+\chi_z^{(-1)}}\ , \quad (14a)$$

the prebunched coefficient is

$$\zeta=\frac{kV_{W_x}}{4\epsilon_0 c V_z\theta_p^2}\ , \quad (14b)$$

and the effective prebunched current is

$$\tilde{J}_{\rm in}=\rho_0\tilde{\tilde{v}}_z-\frac{1}{s}\left[\frac{j\omega}{V_z}+s-jk_W\right]\tilde{J}_{z0}\ . \quad (14c)$$

Equation (13) is solved now by a Fourier transform on the x variable,

$$\hat{E}_x(k_x)=\mathcal{F}(\tilde{\tilde{E}}_x(x))=\int_x\tilde{\tilde{E}}_x(x)\exp(-jk_x x)dx\ .$$

This leads to the algebraic equations

$$\frac{1}{2s}(k^2+s^2-k_x^2)\hat{E}_x(k_x)+j\kappa\hat{D}(k_x)*\hat{E}_x(k_x)$$
$$=\hat{E}_{x0}(k_x)+j\zeta\hat{D}(k_x)*\hat{J}_{\rm in}(k_x)\ , \quad (15)$$

where the $*$ notation denotes the convolution operation in the k_x space. The physical meaning of the convolution in this context is the coupling between the vacuum modes (the plane waves) due to the FEL interaction. Equation (15) is solved by discretizing the k_x dimension. The wave number k_x is replaced by nk_{0x} where k_{0x} is the wave-number resolution. This discretization can be related to the physical transverse dimension of the system, the wiggler gap a for instance, by $k_{0x}=2\pi/a$. The angular spectrum is truncated, taking into account the limited FEL detuning range [which is approximated by $\Delta\bar{\theta}(k_x)\sim\pi$ in the low-gain regime, and by $\Delta\bar{\theta}(k_x)\sim 3\bar{Q}^{1/3}$ in the high-gain regime, where $\bar{Q}=\kappa\theta_p^2 L_W^3$ is the gain parameter[17]]. Equation (15) is written then in the matrix form[18]

$$\underline{E}_{\rm out}=(\underline{\underline{K}}+j\kappa\underline{\underline{D}})^{(-1)}(\underline{E}_{\rm in}+j\zeta\underline{\underline{D}}\,\underline{J}_{\rm in})\ . \quad (16)$$

The vectors $\underline{E}_{\rm out}$, $\underline{E}_{\rm in}$, and $\underline{J}_{\rm in}$ contain the components of the s-dependent output field $\hat{E}_x(nk_{0x},s)$, the input field $\hat{E}_{x0}(nk_{0x},z=0)$, and the input current $\hat{J}_{\rm in}(nk_{0x},z=0)$, respectively. The free-space propagation matrix $\underline{\underline{K}}$ is a diagonal matrix that consists of the elements $[k^2+s^2-(nk_{0x})^2]/2s$. The matrix $\underline{\underline{D}}$ contains the dispersion components $\hat{D}(nk_{0x})$ in a form that the vector results of $\underline{\underline{D}}\,\underline{E}_X$ describes the discretized convolution $\hat{D}(nk_{0x})*\hat{E}_x(nk_{0x})$, as described in Ref. 18.

Equation (16) can be regarded as the matrix transfer function for the prebunched FEL. It describes the output-input relations of the linear interaction in the transformed (ω,s,k_x) space. The radiation pattern in the

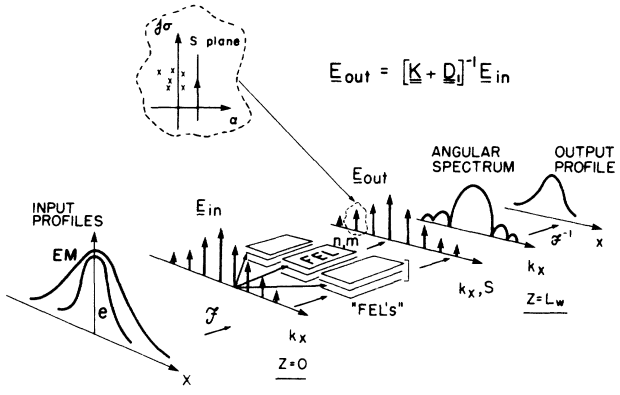

FIG. 4. A figurative description of the matrix gain-dispersion equation (16). The em wave profile and the e-beam profile are presented by their transverse Fourier spectrum. Each component of the em angular spectrum of plane waves interacts with all the others due to the mode coupling caused by the finite transverse e-beam profile. An inverse Laplace transform is performed on each output line to obtain the output angular spectrum components, and the radiation pattern in the far field. The output em wave profile is obtained by an inverse Fourier transform.

far field is obtained from Eq. (16) by performing the inverse Laplace transform on the vector $\underline{E}_{\text{out}}$. This results in the angular spectrum of plane waves $\tilde{E}_x(k_x, z=L_W)$ in the exit plane. The relative angular radiation pattern in the far field, $|E_x(\alpha)|$, is given immediately by the substitution $|\tilde{E}_x(k_x=k_0\sin\alpha)|$.[3] The em wave profile at the FEL exit, $\tilde{E}_x(x, z=L_W)$, is obtained by an inverse Fourier transform on $\tilde{E}_x(k_x)$. A figurative description of the FEL transfer function and the numerical procedure to solve it are shown in Fig. 4. Equation (16) is a 2D expansion of the scalar gain-dispersion equation for the prebunched FEL (Ref. 13) in the form of the matrix 3D equation given in Ref. 18 for the ordinary (nonprebunched) FEL. Numerical solutions of Eq. (16) are presented in the next section.

IV. NUMERICAL EXAMPLES FOR ANGULAR STEERING

The 2D gain-dispersion equation (16) was solved to demonstrate features of the FEL angular steering in the broadside and the end-fire schemes.

The results for the broadside steering schemes are shown in Figs. 5(a) and 5(b). The FEL parameters in this

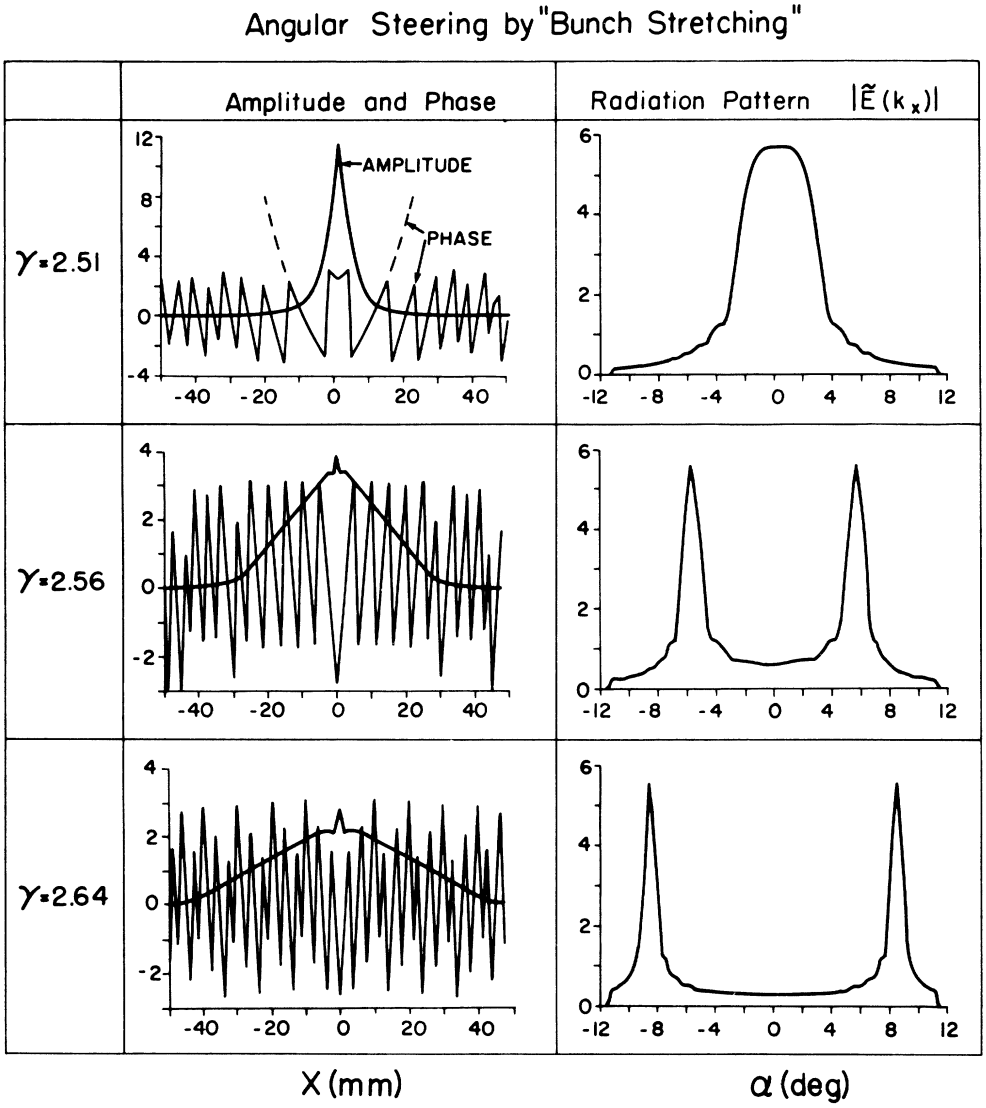

FIG. 5. Angular steering in a "bunch stretching" broadside scheme. The prebunched FEL parameters are $\lambda=0.5$ mn, $\lambda_W=5$ mm, $L_W=0.3$ m, $\bar{a}_W=0.3$, and $\theta_p=0.3$. For $\gamma=2.51$ the FEL is optimally synchronized and the em beam is emitted on axis. Increasing the input prebunched e-beam energy leads to a larger off-axis angle α. The left column shows the relative amplitude in dimensionless units for comparison between the various cases, and the corresponding phase profiles, as functions of x (in millimeters). The right column shows the corresponding radiation patterns as functions of α (in degrees). (b) Angular steering by shortening the wiggler period λ_W in a broadside scheme. The parameters, and the axis units, are the same as in (a) for comparison. Shortening λ_W leads to off-axis radiation.

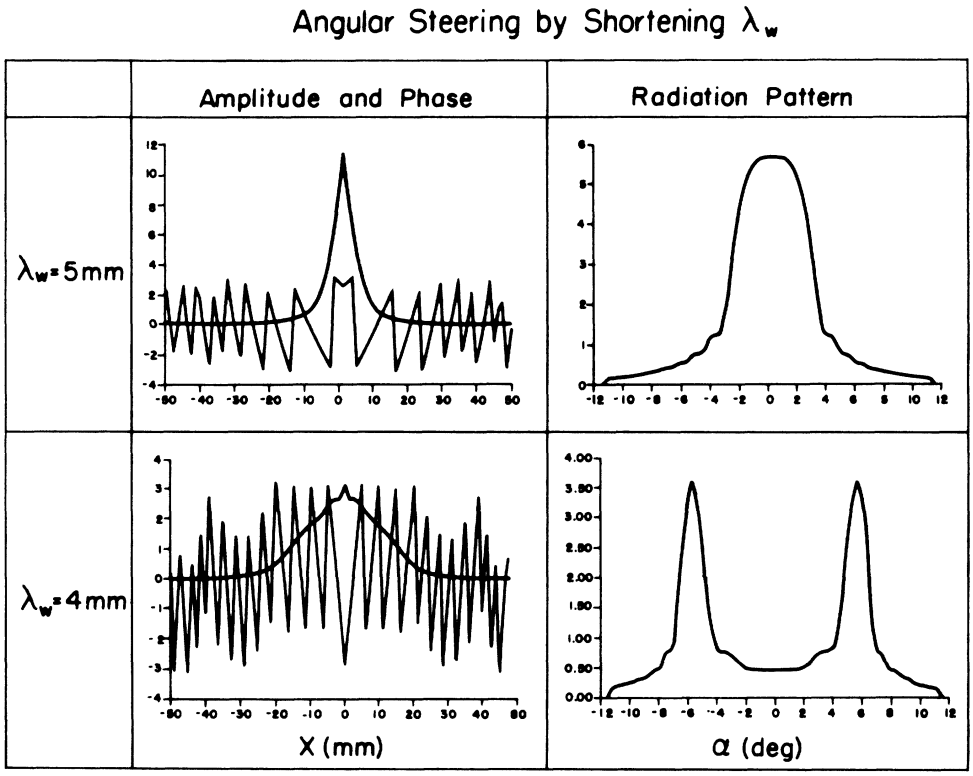

FIG. 5. (*Continued*).

example are $\lambda=0.5$ mm, $\lambda_W=5$ mm, $L_W=0.3$ m, $\bar{a}_W=0.3$, and $\theta_p=0.3$. The wiggler period corresponds to the miniature wiggler devices, presented in Refs. 19 and 20. Profiles of the relative output amplitude and phase (truncated to $\pm\pi$) and of the radiation pattern are shown for comparison. In the conventional case of optimal synchronism ($\gamma=2.51$) the radiation pattern is confined to the FEL axis. By a small increase of the prebunched e-beam energy at the entrance to the radiator ($\gamma=2.56$) the 2D radiation pattern is split to two symmetrical lobes with $\alpha\cong\pm 6°$. In a 3D symmetrical case this effect would yield a conical radiation pattern. Further increase of the energy of the prebunched e beam ($\gamma=2.64$) leads to a greater off-axis angle, $\alpha\cong\pm 8°$. Similar results are obtained for shortening λ_W in the radiator section (instead of accelerating the bunched e beam) as shown in Fig. 5(b). The effect of making the wiggler period in the previous example shorter to $\lambda_W=4$ mm is an off-axis angle of $\alpha\cong\pm 6°$.

Figure 6 shows an example for the high-gain FEL steering in the end-fire scheme. The angular steering is obtained in this case by a linear velocity shear. The FEL parameters in this example are $\lambda=1$ mm, $\lambda_W=2$ cm, $L_W=1$ m, $\bar{a}_W=0.6$, $\gamma=3.8$, and $\theta_p=6$. The right column in Fig. 6 shows the effect of the velocity detuning shear on the output amplitude and phase (truncated to $\pm\pi$), and on the radiation pattern. The detuning shear in this case, $\Delta\bar{\theta}=40$ over the entire e-beam cross section, corresponds to a velocity difference, $\Delta V_z/V_z$, of about 0.6% across the e beam. As a result, the radiation lobe is deviated to $+4°$ off axis. The case of a uniform e-beam velocity is shown for the sake of comparison in the left column of Fig. 6. The amplitude profile is higher and wider here because the entire e-beam cross section participates in the interaction. Consequently, the radiation pattern is narrower and higher than in the right column. These differences could be much smaller if the e-beam width were optimized to the maximum steering limit in this case. The effect of the velocity shear is similar in this aspect to the effect of the velocity spread in a warm e beam. However, the "spread" in this case is ordered and it can be compensated in some cases by an appropriate density shear as was proposed by Fruchtman.[7]

V. LIMITATIONS AND APPLICATIONS OF THE FEL ANGULAR STEERING

The principle limitations of the FEL angular steering can be derived by simple considerations. In the broadside schemes the steering limits are consequences of the modified parameter. The "bunch stretching" method [Fig. 3, row (b)] is limited by the amount of velocity which can be added to the prebunched e beam, since $V_z<c$. This leads directly to the limit

$$\alpha<(2\lambda/\lambda_W)^{1/2}\ . \tag{17a}$$

For the conventional FEL this results in $\alpha\sim 1/\gamma$, the known angular width of the FEL spontaneous emission. This seems to be a narrow steering range for a typical FEL. However, FEL's that employ miniature

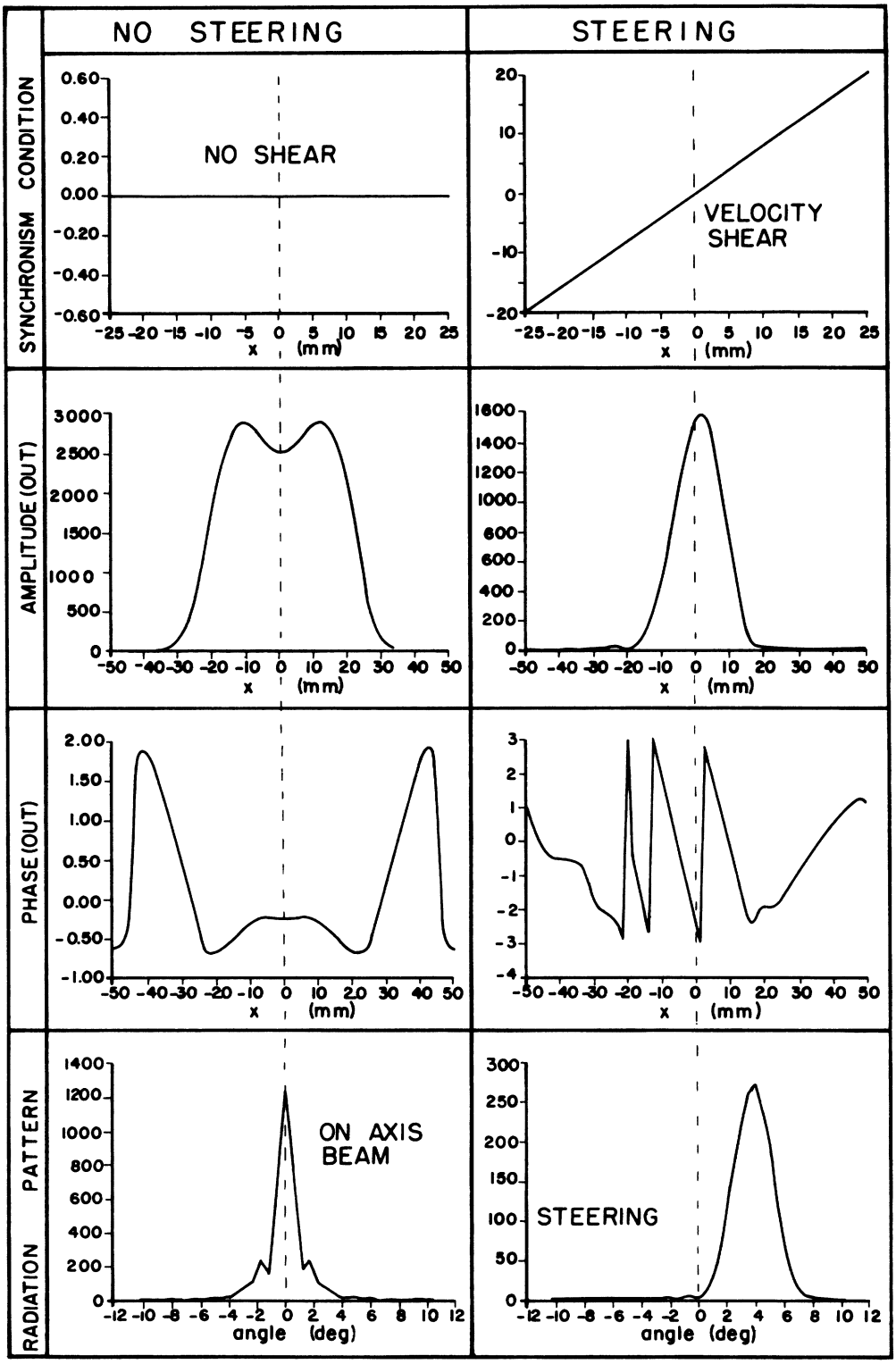

FIG. 6. Angular steering in an end-fire scheme for high-gain FEL's. The FEL parameters are $\lambda=1$ mm, $\lambda_W=2$ cm, $L_W=1$ m, $\bar{a}_W=0.6$, and $\theta_p=6$. The e-beam density is uniform in the range $-25\text{ mm}<x<25$ mm, and is zero elsewhere. By inducing a linear velocity shear, as shown in the right column, the synchronism parameter $\bar{\theta}$ is sheared and consequently the output phase profile (shown here truncated to $\pm\pi$) is sheared. Hence, the radiation beam is emitted off axis. The left column shows the optimal on-axis case for comparison.

wigglers,[19,20] and are operating in the millimeter and submillimeter ranges, may enable a considerable angular steering range. In the example shown in Fig. 5 ($\lambda_W=5$ mm and $\lambda=0.5$ mm) the steering range is within $\pm 20°$. In a case that the ratio λ/λ_W is closer to 1 the steering sector becomes much larger. A similar result is accepted for the other broadside method of shortening the wiggler period [Fig. 3, row (c)]. Defining s as the ratio between the optimal wiggler period ($\alpha=0$) and the shortened period, the off-axis steering angle becomes

$$\alpha \cong [2(s-1)\lambda/\lambda_W]^{1/2} . \tag{17b}$$

For one octave tuning, $s=2$, one gets the same results as in Eq. (17a).

The limit of the angular steering of the end-fire steering in the high-gain regime can be evaluated by the FEL detuning acceptance $\Delta\bar{\theta} \sim 3\bar{Q}^{1/3}$.[17] This leads to a heuristic approximation

$$\alpha_{\max} \sim \frac{\lambda \bar{Q}^{1/3}}{4a_b} , \tag{18}$$

where a_b is the e-beam width, and $\lambda \ll a_b$. For $\bar{Q}=1000$, $\lambda=0.1$ mm, and $a_b=2$ mm the steering range results in approximately $\pm 7°$.

The limitations of the angular steering methods presented in this section are applicable for the linear regime. The evaluation of the FEL efficiency, and the angular steering performances in the saturated regime should be studied by nonlinear models.

The numerical examples shown in Figs. 5 and 6, and the theoretical limits [(17), (18)] show that in the millimeter and the submillimeter range one may expect a considerable angular steering range for FEL's operating in the linear regime. The widest steering range is accepted for the broadside scheme, using a microwiggler.[19,20] However, the end-fire scheme produces non-negligible off-axis steering angles. These results may lead to a variety of applications for the angularly steered FEL.

One possible application for the angularly steered FEL is as a *power divider*. The radiation produced by the FEL can be switched by the angular steering mechanism among various consumers, separated angularly in space. Another application can be for the cavity dumping in a FEL oscillator. The radiation is built up on axis ($\alpha=0$). Then it can be extracted from the cavity by operating the angular steering, as an *angular Q switch*. These applications do not require large steering angles, hence the end-fire scheme can be considered. Finally, the angularly directed FEL can be considered as a hybrid FEL-antenna device. This hybrid device can be useful in a system which requires both functions—production of em waves, and radiating them in a variable direction to the free space. This application may require a relatively wide range of angular steering, which can be satisfied by the broadside schemes.

ACKNOWLEDGMENTS

The author wishes to thank Professor George Bekefi, Professor Avi Gover, Professor Shlomo Ruschin, and Dr. Ammon Fruchtman, for their help. This work was supported in part by the Rothschild and the Fulbright Foundations.

[1]T. C. Marshall, *Free Electron Lasers* (Macmillan, New York, 1985).

[2]For recent FEL studies, see the Proceedings of the FEL Conferences [Nucl. Instrum. Methods A **237** (1985); **250** (1986); **259** (1987); and **272** (1988)].

[3]R. E. Collin, *Antennas and Radiowave Propagation* (McGraw-Hill, New York, 1985).

[4]P. Sprangle, A. Ting, and C. M. Tang, Phys. Rev. Lett. **59**, 202 (1987); also in Phys. Rev. A **36**, 2773 (1987).

[5]W. B. Colson, G. Dattoli, and F. Ciocco, Phys. Rev. A **31**, 828 (1985).

[6]E. T. Scharlemann, A. M. Sessler, and J. S. Wurtele, Phys. Rev. Lett. **54**, 1925 (1985).

[7]A. Fruchtman, Phys. Rev. A **31**, 2989 (1988); for additional studies on this subject see the chapters on optical guiding in Ref. 2.

[8]J. Fajans and G. Bekefi, Phys. Fluids **29**, 3461 (1986).

[9]J. E. LaSala, D. A. G. Deacon, and J. M. J. Madey, Phys. Rev. Lett. **59**, 2047 (1987).

[10]A. Bhattacharjee, S. Y. Cai, S. P. Chang, J. W. Dodd, and T. C. Marshall, Phys. Rev. Lett. **60**, 1254 (1988).

[11]R. Coisson, Part. Accel. **11**, 245 (1981).

[12]B. Girard, Y. Lapierre, J. M. Ortega, C. Bazin, M. Billardon, P. Elleaume, M. Bergher, M. Velghe, and Y. Petroff, Phys. Rev. Lett. **53**, 2405 (1984).

[13]J. Schnitzer and A. Gover, Nucl. Instrum. Methods A **237**, 124 (1985).

[14]C. Leibovitch, K. Xu, and G. Bekefi, IEEE J. Quantum Electron. **24**, 1825 (1988).

[15]J. S. Wurtele, G. Bekefi, R. Chu, and K. Xu, Phys. Fluids B **2**, 401 (1990).

[16]A. Gover and P. Sprangle, IEEE J. Quantum Electron. **QE-17**, 1196 (1981).

[17]E. Jerby and A. Gover, IEEE J. Quantum Electron. **QE-21**, 1041 (1985).

[18]E. Jerby and A. Gover, Phys. Rev. Lett. **63**, 864 (1989).

[19]S. C. Chen, G. Bekefi, S. DiCecca, and R. Temkin, Appl. Phys. Lett. **54**, 1299 (1989), and references therein.

[20]A. Sneh and E. Jerby, Nucl. Instrum. Methods A **285**, 294 (1989).